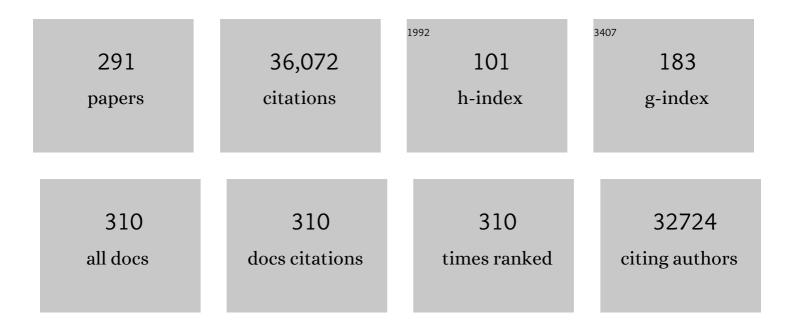
Nan-Feng Zheng

List of Publications by Year in descending order

Source: https://exaly.com/author-pdf/2336732/publications.pdf Version: 2024-02-01



#	Article	IF	CITATIONS
1	Catalysis with two-dimensional materials and their heterostructures. Nature Nanotechnology, 2016, 11, 218-230.	31.5	1,833
2	Photochemical route for synthesizing atomically dispersed palladium catalysts. Science, 2016, 352, 797-800.	12.6	1,540
3	Freestanding palladium nanosheets with plasmonic and catalytic properties. Nature Nanotechnology, 2011, 6, 28-32.	31.5	1,423
4	All-thiol-stabilized Ag44 and Au12Ag32 nanoparticles with single-crystal structures. Nature Communications, 2013, 4, 2422.	12.8	675
5	Interfacial Effects in Iron-Nickel Hydroxide–Platinum Nanoparticles Enhance Catalytic Oxidation. Science, 2014, 344, 495-499.	12.6	591
6	Interfacial electronic effects control the reaction selectivity of platinum catalysts. Nature Materials, 2016, 15, 564-569.	27.5	548
7	The Interface Chemistry between Chalcogenide Clusters and Open Framework Chalcogenides. Accounts of Chemical Research, 2005, 38, 293-303.	15.6	541
8	Surface Coordination Chemistry of Metal Nanomaterials. Journal of the American Chemical Society, 2017, 139, 2122-2131.	13.7	522
9	One-Step One-Phase Synthesis of Monodisperse Noble-Metallic Nanoparticles and Their Colloidal Crystals. Journal of the American Chemical Society, 2006, 128, 6550-6551.	13.7	509
10	Amine-Assisted Synthesis of Concave Polyhedral Platinum Nanocrystals Having {411} High-Index Facets. Journal of the American Chemical Society, 2011, 133, 4718-4721.	13.7	489
11	From Hollow Carbon Spheres to Nâ€Doped Hollow Porous Carbon Bowls: Rational Design of Hollow Carbon Host for Liâ€5 Batteries. Advanced Energy Materials, 2016, 6, 1502539.	19.5	485
12	A General Synthetic Strategy for Oxide-Supported Metal Nanoparticle Catalysts. Journal of the American Chemical Society, 2006, 128, 14278-14280.	13.7	464
13	Surface Chemistry of Atomically Precise Coinage–Metal Nanoclusters: From Structural Control to Surface Reactivity and Catalysis. Accounts of Chemical Research, 2018, 51, 3084-3093.	15.6	459
14	Surface and interface control of noble metal nanocrystals for catalytic and electrocatalytic applications. Nano Today, 2013, 8, 168-197.	11.9	431
15	Small Adsorbateâ€Assisted Shape Control of Pd and Pt Nanocrystals. Advanced Materials, 2012, 24, 862-879.	21.0	415
16	Microporous and Photoluminescent Chalcogenide Zeolite Analogs. Science, 2002, 298, 2366-2369.	12.6	410
17	Synthetic design of crystalline inorganic chalcogenides exhibiting fast-ion conductivity. Nature, 2003, 426, 428-432.	27.8	399
18	Nonaqueous Production of Nanostructured Anatase with High-Energy Facets. Journal of the American Chemical Society, 2008, 130, 17563-17567.	13.7	389

#	Article	IF	CITATIONS
19	Core–Shell Pd@Au Nanoplates as Theranostic Agents for Inâ€Vivo Photoacoustic Imaging, CT Imaging, and Photothermal Therapy. Advanced Materials, 2014, 26, 8210-8216.	21.0	383
20	Efficient, Hysteresisâ€Free, and Stable Perovskite Solar Cells with ZnO as Electronâ€Transport Layer: Effect of Surface Passivation. Advanced Materials, 2018, 30, 1705596.	21.0	363
21	A Two-Dimensional Porous Carbon-Modified Separator for High-Energy-Density Li-S Batteries. Joule, 2018, 2, 323-336.	24.0	344
22	Surface Coordination Chemistry of Atomically Dispersed Metal Catalysts. Chemical Reviews, 2020, 120, 11810-11899.	47.7	325
23	Synthesis of Ultrathin Nitrogen-Doped Graphitic Carbon Nanocages as Advanced Electrode Materials for Supercapacitor. ACS Applied Materials & Interfaces, 2013, 5, 2241-2248.	8.0	320
24	Polypyrrole nanoparticles for high-performance in vivo near-infrared photothermal cancer therapy. Chemical Communications, 2012, 48, 8934.	4.1	319
25	Recent Advances in Hollow Porous Carbon Materials for Lithium–Sulfur Batteries. Small, 2019, 15, e1804786.	10.0	314
26	Facile Synthesis of Manganeseâ€Oxideâ€Containing Mesoporous Nitrogenâ€Doped Carbon for Efficient Oxygen Reduction. Advanced Functional Materials, 2012, 22, 4584-4591.	14.9	306
27	A cationic surfactant assisted selective etching strategy to hollow mesoporous silica spheres. Nanoscale, 2011, 3, 1632.	5.6	303
28	Self-supporting sulfur cathodes enabled by two-dimensional carbon yolk-shell nanosheets for high-energy-density lithium-sulfur batteries. Nature Communications, 2017, 8, 482.	12.8	300
29	Atomically Precise Alkynyl-Protected Metal Nanoclusters as a Model Catalyst: Observation of Promoting Effect of Surface Ligands on Catalysis by Metal Nanoparticles. Journal of the American Chemical Society, 2016, 138, 3278-3281.	13.7	297
30	Subâ€10â€nm Pd Nanosheets with Renal Clearance for Efficient Nearâ€Infrared Photothermal Cancer Therapy. Small, 2014, 10, 3139-3144.	10.0	286
31	Ultrasound-Switchable Nanozyme Augments Sonodynamic Therapy against Multidrug-Resistant Bacterial Infection. ACS Nano, 2020, 14, 2063-2076.	14.6	281
32	Selective Hydrogenation of α,βâ€Unsaturated Aldehydes Catalyzed by Amineâ€Capped Platinumâ€Cobalt Nanocrystals. Angewandte Chemie - International Edition, 2012, 51, 3440-3443.	13.8	277
33	Strategies for Stabilizing Atomically Dispersed Metal Catalysts. Small Methods, 2018, 2, 1700286.	8.6	276
34	Golden single-atomic-site platinum electrocatalysts. Nature Materials, 2018, 17, 1033-1039.	27.5	266
35	Self-templating synthesis of hollow mesoporous silica and their applications in catalysis and drug delivery. Nanoscale, 2013, 5, 2205.	5.6	262
36	One-Pot, High-Yield Synthesis of 5-Fold Twinned Pd Nanowires and Nanorods. Journal of the American Chemical Society, 2009, 131, 4602-4603.	13.7	259

#	Article	IF	CITATIONS
37	Simplifying the Creation of Hollow Metallic Nanostructures: Oneâ€Pot Synthesis of Hollow Palladium/Platinum Singleâ€Crystalline Nanocubes. Angewandte Chemie - International Edition, 2009, 48, 4808-4812.	13.8	258
38	Hollow Mesoporous Aluminosilica Spheres with Perpendicular Pore Channels as Catalytic Nanoreactors. ACS Nano, 2012, 6, 4434-4444.	14.6	253
39	Identifying the Molecular Structures of Intermediates for Optimizing the Fabrication of High-Quality Perovskite Films. Journal of the American Chemical Society, 2016, 138, 9919-9926.	13.7	249
40	Open-Framework Chalcogenides as Visible-Light Photocatalysts for Hydrogen Generation from Water. Angewandte Chemie - International Edition, 2005, 44, 5299-5303.	13.8	248
41	Crystal structure of a luminescent thiolated Ag nanocluster with an octahedral Ag ₆ ⁴⁺ core. Chemical Communications, 2013, 49, 300-302.	4.1	244
42	Uniform Ordered Two-Dimensional Mesoporous TiO ₂ Nanosheets from Hydrothermal-Induced Solvent-Confined Monomicelle Assembly. Journal of the American Chemical Society, 2018, 140, 4135-4143.	13.7	242
43	Enhancing the Photothermal Stability of Plasmonic Metal Nanoplates by a Coreâ€6hell Architecture. Advanced Materials, 2011, 23, 3420-3425.	21.0	240
44	Controlled Formation of Concave Tetrahedral/Trigonal Bipyramidal Palladium Nanocrystals. Journal of the American Chemical Society, 2009, 131, 13916-13917.	13.7	238
45	Tetrahedral Chalcogenide Clusters and Open Frameworks. Chemistry - A European Journal, 2004, 10, 3356-3362.	3.3	235
46	Plasmonic twinned silver nanoparticles with molecular precision. Nature Communications, 2016, 7, 12809.	12.8	235
47	Well-Defined Thiolated Nanographene as Hole-Transporting Material for Efficient and Stable Perovskite Solar Cells. Journal of the American Chemical Society, 2015, 137, 10914-10917.	13.7	229
48	Total Structure and Electronic Structure Analysis of Doped Thiolated Silver [MAg ₂₄ (SR) ₁₈] ^{2–} (M = Pd, Pt) Clusters. Journal of the American Chemical Society, 2015, 137, 11880-11883.	13.7	221
49	Electrochemical Reduction of Carbon Dioxide to Methanol on Hierarchical Pd/SnO ₂ Nanosheets with Abundant Pd–O–Sn Interfaces. Angewandte Chemie - International Edition, 2018, 57, 9475-9479.	13.8	218
50	A Novel Theranostic Nanoplatform Based on Pd@Ptâ€PECâ€Ce6 for Enhanced Photodynamic Therapy by Modulating Tumor Hypoxia Microenvironment. Advanced Functional Materials, 2018, 28, 1706310.	14.9	216
51	In Situ Electrochemical Production of Ultrathin Nickel Nanosheets for Hydrogen Evolution Electrocatalysis. CheM, 2017, 3, 122-133.	11.7	214
52	Ultrastable atomic copper nanosheets for selective electrochemical reduction of carbon dioxide. Science Advances, 2017, 3, e1701069.	10.3	211
53	Facet engineering accelerates spillover hydrogenation on highly diluted metal nanocatalysts. Nature Nanotechnology, 2020, 15, 848-853.	31.5	210
54	Nanoscale engineering of catalytic materials for sustainable technologies. Nature Nanotechnology, 2021, 16, 129-139.	31.5	210

#	Article	IF	CITATIONS
55	Asymmetric Synthesis of Chiral Bimetallic [Ag ₂₈ Cu ₁₂ (SR) ₂₄] ^{4–} Nanoclusters via Ion Pairing. Journal of the American Chemical Society, 2016, 138, 12751-12754.	13.7	196
56	An Assembly Route to Inorganic Catalytic Nanoreactors Containing Subâ€10â€nm Gold Nanoparticles with Antiâ€Aggregation Properties. Small, 2009, 5, 361-365.	10.0	192
57	Pd Nanosheetâ€Covered Hollow Mesoporous Silica Nanoparticles as a Platform for the Chemoâ€Photothermal Treatment of Cancer Cells. Small, 2012, 8, 3816-3822.	10.0	191
58	High-Efficiency, Hysteresis-Less, UV-Stable Perovskite Solar Cells with Cascade ZnO–ZnS Electron Transport Layer. Journal of the American Chemical Society, 2019, 141, 541-547.	13.7	189
59	Photo―and pHâ€Triggered Release of Anticancer Drugs from Mesoporous Silica oated Pd@Ag Nanoparticles. Advanced Functional Materials, 2012, 22, 842-848.	14.9	187
60	Hollow Mesoporous Zirconia Nanocapsules for Drug Delivery. Advanced Functional Materials, 2010, 20, 2442-2447.	14.9	184
61	Thiols as interfacial modifiers to enhance the performance and stability of perovskite solar cells. Nanoscale, 2015, 7, 9443-9447.	5.6	179
62	An Intermetallic Au ₂₄ Ag ₂₀ Superatom Nanocluster Stabilized by Labile Ligands. Journal of the American Chemical Society, 2015, 137, 4324-4327.	13.7	175
63	<scp>I</scp> -DNA Molecular Beacon: A Safe, Stable, and Accurate Intracellular Nano-thermometer for Temperature Sensing in Living Cells. Journal of the American Chemical Society, 2012, 134, 18908-18911.	13.7	173
64	Self‣upported 3D PdCu Alloy Nanosheets as a Bifunctional Catalyst for Electrochemical Reforming of Ethanol. Small, 2017, 13, 1602970.	10.0	168
65	Identifying the electrocatalytic sites of nickel disulfide in alkaline hydrogen evolution reaction. Nano Energy, 2017, 41, 148-153.	16.0	168
66	Ligand-Stabilized Au ₁₃ Cu _{<i>x</i>} (<i>x</i> = 2, 4, 8) Bimetallic Nanoclusters: Ligand Engineering to Control the Exposure of Metal Sites. Journal of the American Chemical Society, 2013, 135, 9568-9571.	13.7	162
67	High Sulfur Loading in Hierarchical Porous Carbon Rods Constructed by Vertically Oriented Porous Grapheneâ€Like Nanosheets for Liâ€ S Batteries. Advanced Functional Materials, 2016, 26, 8952-8959.	14.9	159
68	Interfacing with silica boosts the catalysis of copper. Nature Communications, 2018, 9, 3367.	12.8	159
69	Self-Assembly of Novel Dye Molecules and [Cd8(SPh)12]4+Cubic Clusters into Three-Dimensional Photoluminescent Superlattice. Journal of the American Chemical Society, 2002, 124, 9688-9689.	13.7	157
70	Stabilizing subnanometer Ag(0) nanoclusters by thiolate and diphosphine ligands and their crystal structures. Nanoscale, 2013, 5, 2674.	5.6	154
71	Surface coordination layer passivates oxidation of copper. Nature, 2020, 586, 390-394.	27.8	154
72	A multiple coating route to hollow carbon spheres with foam-like shells and their applications in supercapacitor and confined catalysis. Journal of Materials Chemistry A, 2014, 2, 6191.	10.3	153

#	Article	IF	CITATIONS
73	Robust Lithium Metal Anodes Realized by Lithiophilic 3D Porous Current Collectors for Constructing High-Energy Lithium–Sulfur Batteries. ACS Nano, 2019, 13, 8337-8346.	14.6	152
74	Small molecules control the formation of Pt nanocrystals: a key role of carbon monoxide in the synthesis of Pt nanocubes. Chemical Communications, 2011, 47, 1039-1041.	4.1	150
75	An investigation of the mimetic enzyme activity of two-dimensional Pd-based nanostructures. Nanoscale, 2015, 7, 19018-19026.	5.6	150
76	A General Route to Diverse Mesoporous Metal Oxide Submicrospheres with Highly Crystalline Frameworks. Angewandte Chemie - International Edition, 2008, 47, 8682-8686.	13.8	149
77	Precisely controlled resorcinol–formaldehyde resin coating for fabricating core–shell, hollow, and yolk–shell carbon nanostructures. Nanoscale, 2013, 5, 6908.	5.6	148
78	Structural Evolution of Atomically Precise Thiolated Bimetallic [Au _{12+<i>n</i>} Cu ₃₂ (SR) _{30+<i>n</i>}] ^{4–} (<i>n</i> = 0,) 1	j ETBQ7q0 () 01rgBT /Over
79	Thiol Treatment Creates Selective Palladium Catalysts for Semihydrogenation of Internal Alkynes. CheM, 2018, 4, 1080-1091.	11.7	145
80	Nonaqueous Synthesis and Selective Crystallization of Gallium Sulfide Clusters into Three-Dimensional Photoluminescent Superlattices. Journal of the American Chemical Society, 2003, 125, 1138-1139.	13.7	138
81	Atomically Precise, Thiolated Copper–Hydride Nanoclusters as Single-Site Hydrogenation Catalysts for Ketones in Mild Conditions. ACS Nano, 2019, 13, 5975-5986.	14.6	138
82	Pushing Up the Size Limit of Chalcogenide Supertetrahedral Clusters:Â Two- and Three-Dimensional Photoluminescent Open Frameworks from (Cu5In30S54)13-Clusters. Journal of the American Chemical Society, 2002, 124, 12646-12647.	13.7	137
83	Etching Growth under Surface Confinement: An Effective Strategy To Prepare Mesocrystalline Pd Nanocorolla. Journal of the American Chemical Society, 2011, 133, 15946-15949.	13.7	136
84	Promoting gold nanocatalysts in solvent-free selective aerobic oxidation of alcohols. Chemical Communications, 2007, , 3862.	4.1	126
85	A graphene–platinum nanoparticles–ionic liquid composite catalyst for methanol-tolerant oxygen reduction reaction. Energy and Environmental Science, 2012, 5, 6923.	30.8	126
86	Multifunctional Core–Shell Upconverting Nanoparticles for Imaging and Photodynamic Therapy of Liver Cancer Cells. Chemistry - an Asian Journal, 2012, 7, 830-837.	3.3	126
87	Highly Robust but Surfaceâ€Active: An Nâ€Heterocyclic Carbene‣tabilized Au ₂₅ Nanocluster. Angewandte Chemie - International Edition, 2019, 58, 17731-17735.	13.8	125
88	Bulky Surface Ligands Promote Surface Reactivities of [Ag ₁₄₁ X ₁₂ (S-Adm) ₄₀] ³⁺ (X = Cl, Br, I) Nanoclusters: Models for Multiple-Twinned Nanoparticles. Journal of the American Chemical Society, 2017, 139, 13288-13291.	13.7	124
89	Alkali ions secure hydrides for catalytic hydrogenation. Nature Catalysis, 2020, 3, 703-709.	34.4	123
90	Carbon Monoxide-Assisted Synthesis of Single-Crystalline Pd Tetrapod Nanocrystals through Hydride Formation. Journal of the American Chemical Society, 2012, 134, 7073-7080.	13.7	120

#	Article	IF	CITATIONS
91	Electrochemical Partial Reforming of Ethanol into Ethyl Acetate Using Ultrathin Co ₃ O ₄ Nanosheets as a Highly Selective Anode Catalyst. ACS Central Science, 2016, 2, 538-544.	11.3	120
92	A photoCORM nanocarrier for CO release using NIR light. Chemical Communications, 2015, 51, 2072-2075.	4.1	119
93	Three-Dimensional Superlattices Built from (M4In16S33)10-(M = Mn, Co, Zn, Cd) Supertetrahedral Clusters. Journal of the American Chemical Society, 2001, 123, 11506-11507.	13.7	118
94	Low-Temperature, Highly Selective, Gas-Phase Oxidation of Benzyl Alcohol over Mesoporous K-Cu-TiO ₂ with Stable Copper(I) Oxidation State. Journal of the American Chemical Society, 2009, 131, 15568-15569.	13.7	116
95	Pd@Pt-GOx/HA as a Novel Enzymatic Cascade Nanoreactor for High-Efficiency Starving-Enhanced Chemodynamic Cancer Therapy. ACS Applied Materials & Interfaces, 2020, 12, 51249-51262.	8.0	116
96	Etherâ€Soluble Cu ₅₃ Nanoclusters as an Effective Precursor of Highâ€Quality Cul Films for Optoelectronic Applications. Angewandte Chemie - International Edition, 2019, 58, 835-839.	13.8	115
97	Hollow-in-hollow carbon spheres with hollow foam-like cores for lithium–sulfur batteries. Nano Research, 2015, 8, 2663-2675.	10.4	114
98	Embryonic Growth of Face-Center-Cubic Silver Nanoclusters Shaped in Nearly Perfect Half-Cubes and Cubes. Journal of the American Chemical Society, 2017, 139, 31-34.	13.7	113
99	Silica coating improves the efficacy of Pd nanosheets for photothermal therapy of cancer cells using near infrared laser. Chemical Communications, 2011, 47, 3948.	4.1	111
100	From Racemic Metal Nanoparticles to Optically Pure Enantiomers in One Pot. Journal of the American Chemical Society, 2017, 139, 16113-16116.	13.7	111
101	Nanocluster with One Missing Core Atom:  A Three-Dimensional Hybrid Superlattice Built from Dual-Sized Supertetrahedral Clusters. Journal of the American Chemical Society, 2002, 124, 10268-10269.	13.7	106
102	Insights into the Interfacial Effects in Heterogeneous Metal Nanocatalysts toward Selective Hydrogenation. Journal of the American Chemical Society, 2021, 143, 4483-4499.	13.7	106
103	Crystalline Superlattices from Single-Sized Quantum Dots. Journal of the American Chemical Society, 2005, 127, 11963-11965.	13.7	105
104	Synthesis of magnetic, fluorescent and mesoporous core-shell-structured nanoparticles for imaging, targeting and photodynamic therapy. Journal of Materials Chemistry, 2011, 21, 11244.	6.7	101
105	Sulfonate-Assisted Surface Iodide Management for High-Performance Perovskite Solar Cells and Modules. Journal of the American Chemical Society, 2021, 143, 10624-10632.	13.7	101
106	Shape ontrolled Synthesis of Surfaceâ€Clean Ultrathin Palladium Nanosheets by Simply Mixing a Dinuclear Pd ^I Carbonyl Chloride Complex with H ₂ O. Angewandte Chemie - International Edition, 2013, 52, 8368-8372.	13.8	100
107	Palladium nanosheets as highly stable and effective contrast agents for in vivo photoacoustic molecular imaging. Nanoscale, 2014, 6, 1271-1276.	5.6	97
108	Multifunctional ultrasmall Pd nanosheets for enhanced near-infrared photothermal therapy and chemotherapy of cancer. Nano Research, 2015, 8, 165-174.	10.4	96

#	Article	IF	CITATIONS
109	Co-crystallization of atomically precise metal nanoparticles driven by magic atomic and electronic shells. Nature Communications, 2018, 9, 3357.	12.8	95
110	One-Dimensional Assembly of Chalcogenide Nanoclusters with Bifunctional Covalent Linkers. Journal of the American Chemical Society, 2005, 127, 14990-14991.	13.7	94
111	Chemoselective Hydrogenation of Nitroaromatics at the Nanoscale Iron(III)–OH–Platinum Interface. Angewandte Chemie - International Edition, 2020, 59, 12736-12740.	13.8	94
112	Single rystalline Rhodium Nanosheets with Atomic Thickness. Advanced Science, 2015, 2, 1500100.	11.2	93
113	Improved stability of perovskite solar cells in ambient air by controlling the mesoporous layer. Journal of Materials Chemistry A, 2015, 3, 16860-16866.	10.3	92
114	Solvent-mediated assembly of atom-precise gold–silver nanoclusters to semiconducting one-dimensional materials. Nature Communications, 2020, 11, 2229.	12.8	91
115	Controlling Bioprocesses with Inorganic Surfaces:  Layered Clay Hemostatic Agents. Chemistry of Materials, 2007, 19, 4390-4392.	6.7	90
116	Assembled molecular face-rotating polyhedra to transfer chirality from two to three dimensions. Nature Communications, 2016, 7, 12469.	12.8	90
117	Microporous Cyclic Titaniumâ€Oxo Clusters with Labile Surface Ligands. Angewandte Chemie - International Edition, 2017, 56, 16252-16256.	13.8	90
118	Templated Assembly of Sulfide Nanoclusters into Cubic-C3N4 Type Framework. Journal of the American Chemical Society, 2003, 125, 6024-6025.	13.7	88
119	From Symmetry Breaking to Unraveling the Origin of the Chirality of Ligated Au ₁₃ Cu ₂ Nanoclusters. Angewandte Chemie - International Edition, 2018, 57, 3421-3425.	13.8	88
120	Fiber network composed of interconnected yolk-shell carbon nanospheres for high-performance lithium-sulfur batteries. Nano Energy, 2018, 54, 50-58.	16.0	87
121	High-yield synthesis and crystal structure of a green Au ₃₀ cluster co-capped by thiolate and sulfide. Chemical Communications, 2014, 50, 14325-14327.	4.1	86
122	A cake making strategy to prepare reduced graphene oxide wrapped plant fiber sponges for high-efficiency solar steam generation. Journal of Materials Chemistry A, 2018, 6, 14571-14576.	10.3	84
123	Superatomic Au13 clusters ligated by different N-heterocyclic carbenes and their ligand-dependent catalysis, photoluminescence, and proton sensitivity. Nano Research, 2020, 13, 1908-1911.	10.4	84
124	Carbon Monoxide-Assisted Synthesis of Ultrathin PtCu ₃ Alloy Wavy Nanowires and Their Enhanced Electrocatalysis. Small, 2016, 12, 1572-1577.	10.0	82
125	A vicinal effect for promoting catalysis of Pd1/TiO2: supports of atomically dispersed catalysts play more roles than simply serving as ligands. Science Bulletin, 2018, 63, 675-682.	9.0	80
126	C ₂ H ₂ Treatment as a Facile Method to Boost the Catalysis of Pd Nanoparticulate Catalysts. Journal of the American Chemical Society, 2014, 136, 5583-5586.	13.7	79

#	Article	IF	CITATIONS
127	Metal-Chelate Dye-Controlled Organization of Cd32S14(SPh)404-Nanoclusters into Three-Dimensional Molecular and Covalent Open Architecture. Journal of the American Chemical Society, 2006, 128, 4528-4529.	13.7	78
128	Carbon monoxide-controlled synthesis of surface-clean Pt nanocubes with high electrocatalytic activity. Chemical Communications, 2012, 48, 2758.	4.1	77
129	Vapor-assisted crystallization control toward high performance perovskite photovoltaics with over 18% efficiency in the ambient atmosphere. Journal of Materials Chemistry A, 2016, 4, 13203-13210.	10.3	77
130	Structure and formation of highly luminescent protein-stabilized gold clusters. Chemical Science, 2018, 9, 2782-2790.	7.4	76
131	A Multiâ€Yolk–Shell Structured Nanocatalyst Containing Subâ€10 nm Pd Nanoparticles in Porous CeO ₂ . ChemCatChem, 2012, 4, 1578-1586.	3.7	75
132	Optimization of Surface Coating on Small Pd Nanosheets for in Vivo near-Infrared Photothermal Therapy of Tumor. ACS Applied Materials & Interfaces, 2015, 7, 14369-14375.	8.0	74
133	Pentasupertetrahedral Clusters as Building Blocks for a Three-Dimensional Sulfide Superlattice. Angewandte Chemie - International Edition, 2004, 43, 4753-4755.	13.8	73
134	[Cu ₃₂ (PET) ₂₄ H ₈ Cl ₂](PPh ₄) ₂ : A Copper Hydride Nanocluster with a Bisquare Antiprismatic Core. Journal of the American Chemical Society, 2020, 142, 13974-13981.	13.7	73
135	Combinatorial Identification of Hydrides in a Ligated Ag ₄₀ Nanocluster with Noncompact Metal Core. Journal of the American Chemical Society, 2019, 141, 11905-11911.	13.7	72
136	Cd ₁₂ Ag ₃₂ (SePh) ₃₆ : Non-Noble Metal Doped Silver Nanoclusters. Journal of the American Chemical Society, 2019, 141, 8422-8425.	13.7	71
137	Surface Coordination of Multiple Ligands Endows Nâ€Heterocyclic Carbeneâ€Stabilized Gold Nanoclusters with High Robustness and Surface Reactivity. Angewandte Chemie - International Edition, 2021, 60, 3752-3758.	13.8	71
138	Interfacial Effects in PdAg Bimetallic Nanosheets for Selective Dehydrogenation of Formic Acid. ChemNanoMat, 2016, 2, 28-32.	2.8	70
139	Titanium–oxo cluster reinforced gel polymer electrolyte enabling lithium–sulfur batteries with high gravimetric energy densities. Energy and Environmental Science, 2021, 14, 975-985.	30.8	69
140	Au/Pt and Au/Pt3Ni nanowires as self-supported electrocatalysts with high activity and durability for oxygen reduction. Chemical Communications, 2011, 47, 11624.	4.1	68
141	Zero- and Two-Dimensional Organization of Tetrahedral Cadmium Chalcogenide Clusters with Bifunctional Covalent Linkers. Chemistry of Materials, 2006, 18, 4307-4311.	6.7	67
142	Interfacial activation of catalytically inert Au (6.7 nm)-Fe3O4 dumbbell nanoparticles for CO oxidation. Nano Research, 2009, 2, 975-983.	10.4	66
143	Electrostatic Self-Assembling Formation of Pd Superlattice Nanowires from Surfactant-Free Ultrathin Pd Nanosheets. Journal of the American Chemical Society, 2014, 136, 12856-12859.	13.7	66
144	A 3D Open–Framework Indium Telluride and Its Selenide and Sulfide Analogues We thank UC Riverside, UC Energy Institute, and the donors of The Petroleum Research Fund (administered by the ACS) for funding Angewandte Chemie - International Edition, 2002, 41, 1959.	13.8	65

#	Article	IF	CITATIONS
145	Three-Dimensional Frameworks of Gallium Selenide Supertetrahedral Clusters. Angewandte Chemie - International Edition, 2004, 43, 1502-1505.	13.8	65
146	Safety profile of two-dimensional Pd nanosheets for photothermal therapy and photoacoustic imaging. Nano Research, 2017, 10, 1234-1248.	10.4	65
147	Stable Nanoâ€Encapsulation of Lithium Through Seedâ€Free Selective Deposition for Highâ€Performance Li Battery Anodes. Advanced Energy Materials, 2020, 10, 1902956.	19.5	65
148	Thiol-stabilized atomically precise, superatomic silver nanoparticles for catalysing cycloisomerization of alkynyl amines. National Science Review, 2018, 5, 694-702.	9.5	63
149	Hierarchical porous carbon microrods composed of vertically aligned graphene-like nanosheets for Li-ion batteries. Journal of Materials Chemistry A, 2015, 3, 19800-19806.	10.3	62
150	Moisture-tolerant and high-quality α-CsPbI ₃ films for efficient and stable perovskite solar modules. Journal of Materials Chemistry A, 2020, 8, 9597-9606.	10.3	62
151	One-dimensional coordination polymers containing penta-supertetrahedral sulfide clusters linked by dipyridyl ligands. Chemical Communications, 2005, , 4916.	4.1	61
152	Platinum(<scp>iv</scp>) prodrug conjugated Pd@Au nanoplates for chemotherapy and photothermal therapy. Nanoscale, 2016, 8, 5706-5713.	5.6	61
153	Site Preference in Multimetallic Nanoclusters: Incorporation of Alkali Metal Ions or Copper Atoms into the Alkynylâ€Protected Bodyâ€Centered Cubic Cluster [Au ₇ Ag ₈ (Câ‰iC ^{<i>t</i>} Bu) ₁₂] ⁺ . Angewandte Chemie - International Edition. 2016. 55. 15152-15156.	13.8	60
154	Coordination chemistry of atomically dispersed catalysts. National Science Review, 2018, 5, 636-638.	9.5	60
155	Iceâ€Templating of Core/Shell Microgel Fibers through †Bricksâ€andâ€Mortar' Assembly**. Advanced Materials, 2007, 19, 4539-4543.	21.0	59
156	Preparation and photodynamic therapy application of NaYF4:Yb, Tm–NaYF4:Yb, Er multifunctional upconverting nanoparticles. New Journal of Chemistry, 2013, 37, 1782.	2.8	59
157	Methylamine-Dimer-Induced Phase Transition toward MAPbI ₃ Films and High-Efficiency Perovskite Solar Modules. Journal of the American Chemical Society, 2020, 142, 6149-6157.	13.7	59
158	Perovskite Quantum Dots as Multifunctional Interlayers in Perovskite Solar Cells with Dopant-Free Organic Hole Transporting Layers. Journal of the American Chemical Society, 2021, 143, 5855-5866.	13.7	59
159	Palladium-based nanomaterials for cancer imaging and therapy. Theranostics, 2020, 10, 10057-10074.	10.0	58
160	Superparamagnetic core-shell polymer particles for efficient purification of his-tagged proteins. Journal of Materials Chemistry, 2010, 20, 8624.	6.7	56
161	Solvent effect on the synthesis of monodisperse amine-capped Au nanoparticles. Chinese Chemical Letters, 2013, 24, 457-462.	9.0	55
162	Cadmiumâ^'Porphyrin Coordination Networks: Rich Coordination Modes and Three-Dimensional Four-Connected CdSO4and (3,5)-Connected hms Nets. Crystal Growth and Design, 2007, 7, 2576-2581.	3.0	54

#	Article	IF	CITATIONS
163	Assembly of Chiral Cluster-Based Metal–Organic Frameworks and the Chirality Memory Effect during their Disassembly. Journal of the American Chemical Society, 2021, 143, 10214-10220.	13.7	54
164	Two-dimensional organization of [ZnGe3S9(H2O)]4– supertetrahedral clusters templated by a metal complex. Chemical Communications, 2005, , 2805.	4.1	53
165	A trustworthy CpG nanoplatform for highly safe and efficient cancer photothermal combined immunotherapy. Nanoscale, 2020, 12, 3916-3930.	5.6	52
166	N-heterocyclic carbene coordinated metal nanoparticles and nanoclusters. Coordination Chemistry Reviews, 2022, 458, 214425.	18.8	52
167	Indium selenide superlattices from (In10Se18)6– supertetrahedral clusters. Chemical Communications, 2002, , 1344-1345.	4.1	51
168	N-Heterocyclic Carbene-Stabilized Gold Nanoclusters with Organometallic Motifs for Promoting Catalysis. Journal of the American Chemical Society, 2022, 144, 10844-10853.	13.7	51
169	Crown Etherâ€Assisted Growth and Scaling Up of FACsPbI ₃ Films for Efficient and Stable Perovskite Solar Modules. Advanced Functional Materials, 2021, 31, 2008760.	14.9	50
170	Pd nanosheets with their surface coordinated byÂradioactive iodide as a high-performance theranostic nanoagent for orthotopic hepatocellular carcinoma imaging and cancer therapy. Chemical Science, 2018, 9, 4268-4274.	7.4	48
171	Lithiophilic and Antioxidative Copper Current Collectors for Highly Stable Lithium Metal Batteries. Advanced Functional Materials, 2021, 31, 2009805.	14.9	47
172	[Pt ₂ Cu ₃₄ (PET) ₂₂ Cl ₄] ^{2–} : An Atomically Precise, 10-Electron PtCu Bimetal Nanocluster with a Direct Pt–Pt Bond. Journal of the American Chemical Society, 2021, 143, 12100-12107.	13.7	47
173	Carbonâ€Monoxideâ€Assisted Synthesis of Ultrathin PtCu Alloy Nanosheets and Their Enhanced Catalysis. ChemNanoMat, 2016, 2, 776-780.	2.8	46
174	Economizing Production of Diverse 2D Layered Metal Hydroxides for Efficient Overall Water Splitting. Small, 2018, 14, e1800759.	10.0	46
175	Two-dimensional Pd-based nanomaterials for bioapplications. Science Bulletin, 2017, 62, 579-588.	9.0	45
176	Shape transformation from Pt nanocubes to tetrahexahedra with size near 10nm. Electrochemistry Communications, 2012, 22, 61-64.	4.7	44
177	Two-dimensional antibacterial Pd@Ag nanosheets with a synergetic effect of plasmonic heating and Ag ⁺ release. Journal of Materials Chemistry B, 2015, 3, 6255-6260.	5.8	43
178	Enhanced Surface Ligands Reactivity of Metal Clusters by Bulky Ligands for Controlling Optical and Chiral Properties. Angewandte Chemie - International Edition, 2021, 60, 12897-12903.	13.8	42
179	Improving Efficiency and Stability of Perovskite Solar Cells by Modifying Mesoporous TiO ₂ –Perovskite Interfaces with Both Aminocaproic and Caproic acids. Advanced Materials Interfaces, 2017, 4, 1700897.	3.7	41
180	Cu2O-Supported Atomically Dispersed Pd Catalysts for Semihydrogenation of Terminal Alkynes: Critical Role of Oxide Supports. CCS Chemistry, 2019, 1, 207-214.	7.8	41

#	Article	IF	CITATIONS
181	Local Structure, Electronic Behavior, and Electrocatalytic Reactivity of CO-Reduced Platinum–Iron Oxide Nanoparticles. Journal of Physical Chemistry C, 2013, 117, 26324-26333.	3.1	40
182	Br-containing alkyl ammonium salt-enabled scalable fabrication of high-quality perovskite films for efficient and stable perovskite modules. Journal of Materials Chemistry A, 2019, 7, 26849-26857.	10.3	40
183	Na5(In4S)(InS4)3·6H2O, a Zeolite-like Structure with Unusual SIn4Tetrahedra. Journal of the American Chemical Society, 2005, 127, 5286-5287.	13.7	39
184	Facile synthesis of size-tunable ZIF-8 nanocrystals using reverse micelles as nanoreactors. Science China Chemistry, 2014, 57, 141-146.	8.2	39
185	Highly Robust but Surfaceâ€Active: An Nâ€Heterocyclic Carbeneâ€Stabilized Au ₂₅ Nanocluster. Angewandte Chemie, 2019, 131, 17895-17899.	2.0	39
186	pH-sensitive radiolabeled and superfluorinated ultra-small palladium nanosheet as a high-performance multimodal platform for tumor theranostics. Biomaterials, 2018, 179, 134-143.	11.4	38
187	Singleâ€6ite Ruthenium Pincer Complex Knitted into Porous Organic Polymers for Dehydrogenation of Formic Acid. ChemSusChem, 2018, 11, 3591-3598.	6.8	36
188	A Novel Cascade Nanoreactor Integrating Twoâ€Đimensional Pdâ€Ru Nanozyme, Uricase and Red Blood Cell Membrane for Highly Efficient Hyperuricemia Treatment. Small, 2021, 17, e2103645.	10.0	36
189	Near-infrared light-triggered irreversible aggregation of poly(oligo(ethylene glycol)) Tj ETQq1 1 0.784314 rgBT /Ov Communications, 2013, 49, 10525.	verlock 10 4.1	Tf 50 427 T 35
190	Amphiphilic modification and asymmetric silica encapsulation of hydrophobic Au–Fe ₃ O ₄ dumbbell nanoparticles. Chemical Communications, 2014, 50, 174-176.	4.1	35
191	Copper-hydride nanoclusters with enhanced stability by N-heterocyclic carbenes. Nano Research, 2021, 14, 3303-3308.	10.4	33
192	Ag ₄₄ (EBT) ₂₆ (TPP) ₄ Nanoclusters With Tailored Molecular and Electronic Structure. Angewandte Chemie - International Edition, 2021, 60, 9038-9044.	13.8	33
193	Origin of the facet dependence in the hydrogenation catalysis of olefins: experiment and theory. Chemical Communications, 2015, 51, 12016-12019.	4.1	32
194	Simple and Selective Synthesis of Copperâ€Containing Metal Nanoclusters Using (PPh ₃) ₂ CuBH ₄ as Reducing Agent. Small Methods, 2021, 5, e2000603.	8.6	32
195	Polyethylene glycol phospholipids encapsulated silicon 2,3-naphthalocyanine dihydroxide nanoparticles (SiNcOH-DSPE-PEC(NH 2) NPs) for single NIR laser induced cancer combination therapy. Chinese Chemical Letters, 2017, 28, 1290-1299.	9.0	31
196	Supercubes, Supersquares, and Superrods of Face-Centered Cubes (FCC): Atomic and Electronic Requirements of [M _{<i>m</i>} (SR) _{<i>l</i>} (PR′ ₃) ₈] ^{<i>q</i>} Nanoclusters (M = Coinage Metals) and Their Implications with Respect to Nucleation and Growth of	4.0	29
197	FCC Metals. Inorganic Chemistry, 2017, 56, 11470-11479. Preface: single-atom catalysts as a new generation of heterogeneous catalysts. National Science Review, 2018, 5, 625-625.	9.5	29
198	Supported monodisperse Pt nanoparticles from [Pt3(CO)3(μ2-CO)3]52â~' clusters for investigating support–Pt interface effect in catalysis. Dalton Transactions, 2013, 42, 12699.	3.3	27

#	Article	IF	CITATIONS
199	Diethyldithiocarbamate-copper nanocomplex reinforces disulfiram chemotherapeutic efficacy through light-triggered nuclear targeting. Theranostics, 2020, 10, 6384-6398.	10.0	27
200	Real-space imaging with pattern recognition of a ligand-protected Ag374 nanocluster at sub-molecular resolution. Nature Communications, 2018, 9, 2948.	12.8	26
201	<i>N</i> -Methyl-2-pyrrolidone as an excellent coordinative additive with a wide operating range for fabricating high-quality perovskite films. Inorganic Chemistry Frontiers, 2019, 6, 2458-2463.	6.0	26
202	Light absorption enhancement by embedding submicron scattering TiO ₂ nanoparticles in perovskite solar cells. RSC Advances, 2016, 6, 24596-24602.	3.6	25
203	Shaping the selectivity in heterogeneous hydrogenation by using molecular modification strategies: Experiment and theory. Catalysis Today, 2017, 279, 36-44.	4.4	25
204	Trace surface-clean palladium nanosheets as a conductivity enhancer in hole-transporting layers to improve the overall performances of perovskite solar cells. Nanoscale, 2016, 8, 3274-3277.	5.6	24
205	Electrochemical Reduction of Carbon Dioxide to Methanol on Hierarchical Pd/SnO ₂ Nanosheets with Abundant Pd–O–Sn Interfaces. Angewandte Chemie, 2018, 130, 9619-9623.	2.0	24
206	Tertiary Chiral Nanostructures from Câ^'Hâ‹â‹F Directed Assembly of Chiroptical Superatoms. Angewandte Chemie - International Edition, 2021, 60, 22411-22416.	13.8	24
207	From Symmetry Breaking to Unraveling the Origin of the Chirality of Ligated Au ₁₃ Cu ₂ Nanoclusters. Angewandte Chemie, 2018, 130, 3479-3483.	2.0	23
208	Intermediate Chemistry of Halide Perovskites: Origin, Evolution, and Application. Journal of Physical Chemistry Letters, 2022, 13, 1765-1776.	4.6	23
209	A hydride-induced-reduction strategy for fabricating palladium-based core–shell bimetallic nanocrystals. Nanoscale, 2014, 6, 6798.	5.6	22
210	Chemical Insights into Interfacial Effects in Inorganic Nanomaterials. Advanced Materials, 2021, 33, e2006159.	21.0	22
211	Atomic overlayer of permeable microporous cuprous oxide on palladium promotes hydrogenation catalysis. Nature Communications, 2022, 13, 2597.	12.8	22
212	The effects of surface ligands and counter cations on the stability of anionic thiolated M12Ag32 (M=Au, Ag) nanoclusters. Chinese Chemical Letters, 2014, 25, 839-843.	9.0	21
213	The biodistribution, excretion and potential toxicity of different-sized Pd nanosheets in mice following oral and intraperitoneal administration. Biomaterials Science, 2017, 5, 2448-2455.	5.4	21
214	Photochemical route for preparing atomically dispersed Pd 1 /TiO 2 catalysts on (001)-exposed anatase nanocrystals and P25. Chinese Journal of Catalysis, 2017, 38, 1574-1580.	14.0	21
215	Microporous Cyclic Titaniumâ€Oxo Clusters with Labile Surface Ligands. Angewandte Chemie, 2017, 129, 16470-16474.	2.0	21
216	A Pd corolla–human serum albumin–indocyanine green nanocomposite for photothermal/photodynamic combination therapy of cancer. Journal of Materials Chemistry B, 2018, 6, 6969-6976.	5.8	21

#	Article	IF	CITATIONS
217	Engineering O–O Species in Boron Nitrous Nanotubes Increases Olefins for Propane Oxidative Dehydrogenation. Journal of the American Chemical Society, 2022, 144, 5930-5936.	13.7	21
218	Antioxidant high-conductivity copper paste for low-cost flexible printed electronics. Npj Flexible Electronics, 2022, 6, .	10.7	21
219	Etherâ€Soluble Cu 53 Nanoclusters as an Effective Precursor of Highâ€Quality Cul Films for Optoelectronic Applications. Angewandte Chemie, 2018, 131, 845.	2.0	20
220	Adhesion of Bacteria to a Graphene Oxide Film. ACS Applied Bio Materials, 2020, 3, 704-712.	4.6	19
221	Regioselective hydrogenation of alkenes over atomically dispersed Pd sites on NHC-stabilized bimetallic nanoclusters. CheM, 2022, 8, 2380-2392.	11.7	19
222	Two distinctive energy migration pathways of monolayer molecules on metal nanoparticle surfaces. Nature Communications, 2016, 7, 10749.	12.8	18
223	The biobehavior, biocompatibility and theranostic application of SPNS and Pd@Au nanoplates in rats and rabbits. Chemical Science, 2019, 10, 1677-1686.	7.4	18
224	Palladium nanoplates scotch breast cancer lung metastasis by constraining epithelial-mesenchymal transition. National Science Review, 2021, 8, .	9.5	18
225	Peculiar holes on checkerboard facets of a trigonal prismatic Au ₉ Ag ₃₆ (SPhCl ₂) ₂₇ (PPh ₃) ₆ cluste caused by steric hindrance and magic electron count. Dalton Transactions, 2017, 46, 1757-1760.	er3.3	17
226	Growth-Dynamic-Controllable Rapid Crystallization Boosts the Perovskite Photovoltaics' Robust Preparation: From Blade Coating to Painting. ACS Applied Materials & Interfaces, 2018, 10, 23103-23111.	8.0	17
227	Solubilityâ€Driven Isolation of a Metastable Nonagold Cluster with Bodyâ€Centered Cubic Structure. Chemistry - A European Journal, 2020, 26, 8465-8470.	3.3	17
228	Heterogeneous Isomerization for Stereoselective Alkyne Hydrogenation to <i>trans</i> -Alkene Mediated by Frustrated Hydrogen Atoms. Journal of the American Chemical Society, 2021, 143, 15882-15890.	13.7	17
229	Robust Roomâ€Temperature Sodiumâ€Sulfur Batteries Enabled by a Sandwichâ€Structured MXene@C/Polyolefin/MXene@C Dualâ€functional Separator. Small, 2022, 18, e2106983.	10.0	17
230	Synergistic Effect between NiO <i>_x</i> and P3HT Enabling Efficient and Stable Hole Transport Pathways for Regular Perovskite Photovoltaics. Advanced Functional Materials, 2022, 32, .	14.9	17
231	Molecular imaging of advanced atherosclerotic plaques with folate receptor-targeted 2D nanoprobes. Nano Research, 2020, 13, 173-182.	10.4	16
232	Carbon Deposition on Heterogeneous Pt Catalysts Promotes the Selective Hydrogenation of Halogenated Nitroaromatics. ACS Applied Materials & Interfaces, 2021, 13, 52193-52201.	8.0	16
233	Bromideâ€Induced Formation of a Highly Symmetric Silver Thiolate Cluster Containing 36 Silver Atoms from an Infinite Polymeric Silver Thiolate. European Journal of Inorganic Chemistry, 2010, 2010, 2010, 2084-2087.	2.0	15
234	Beyond efficiency: phenothiazine, a new commercially viable substituent for hole transport materials in perovskite solar cells. Journal of Materials Chemistry C, 2019, 7, 8593-8598.	5.5	15

#	Article	IF	CITATIONS
235	Amphiphilic silver nanoclusters show active nano–bio interaction with compelling antibacterial activity against multidrug-resistant bacteria. NPG Asia Materials, 2020, 12, .	7.9	15
236	Surface Coordination of Multiple Ligands Endows Nâ€Heterocyclic Carbene‣tabilized Gold Nanoclusters with High Robustness and Surface Reactivity. Angewandte Chemie, 2021, 133, 3796-3802.	2.0	14
237	Advanced nanomaterials for energy conversion and storage: current status and future opportunities. Nanoscale, 2021, 13, 9904-9907.	5.6	14
238	Carbon Monoxide Promotes the Catalytic Hydrogenation on Metal Cluster Catalysts. Research, 2020, 2020, 4172794.	5.7	14
239	Cu ₂₈ H ₂₀ : a peculiar chiral nanocluster with an exposed Cu atom and 13 surface hydrides. Chemical Communications, 2022, 58, 7670-7673.	4.1	14
240	Effect of glutathione on in vivo biodistribution and clearance of surface-modified small Pd nanosheets. Science China Chemistry, 2015, 58, 1753-1758.	8.2	13
241	Fractal Patterns in Nucleation and Growth of Icosahedral Core of [Au _{<i><i>n</i></i>} Ag _{44â€"<i><i>n</i></i>} 6H ₃ F _{2< (<i>n</i>= 0â€"12) via <i>ab Initio</i> Synthesis: Continuously Tunable Composition Control. Inorganic Chemistry, 2019, 58, 259-264.}	/sub>) <su 4.0</su 	b>30^{3}
242	Hyperstable Perovskite Solar Cells Without Ion Migration and Metal Diffusion Based on ZnS Segregated Cubic ZnTiO ₃ Electron Transport Layers. Solar Rrl, 2021, 5, 2000654.	5.8	13
243	Atomically Precise Alkynyl- and Halide-Protected AuAg Nanoclusters Au78Ag66(Câ‰;CPh)48Cl8 and Au74Ag60(Câ‰;CPh)40Br12: The Ligation Effects of Halides. Inorganic Chemistry, 2021, 60, 3529-3533.	4.0	13
244	Scalable Preparation of Highâ€Performance ZnO–SnO ₂ Cascaded Electron Transport Layer for Efficient Perovskite Solar Modules. Solar Rrl, 2022, 6, 2100639.	5.8	13
245	Atomically dispersed palladium catalyzes H/D exchange and isomerization of alkenes via reversible insertion and elimination. Chem Catalysis, 2021, 1, 1480-1492.	6.1	13
246	Preparation of Two-Dimensional Pd@Ir Nanosheets and Application in Bacterial Infection Treatment by the Generation of Reactive Oxygen Species. ACS Applied Materials & amp; Interfaces, 2022, 14, 23194-23205.	8.0	13
247	An iron silicate based pH-sensitive drug delivery system utilizing coordination bonding. Journal of Materials Chemistry B, 2013, 1, 2837.	5.8	12
248	Interface Engineering of Cubic Zinc Metatitanate as an Excellent Electron Transport Material for Stable Perovskite Solar Cells. Solar Rrl, 2020, 4, 1900533.	5.8	12
249	Hexagonal Nickel as a Highly Durable and Active Catalyst for Hydrogen Evolution. ACS Catalysis, 2021, 11, 8798-8806.	11.2	12
250	Site Preference in Multimetallic Nanoclusters: Incorporation of Alkali Metal Ions or Copper Atoms into the Alkynylâ€Protected Bodyâ€Centered Cubic Cluster [Au ₇ Ag ₈ (C≡C ^{<i>t</i>} Bu) ₁₂] ⁺ . Angewandte Chemie, 2016, 128, 15376-15380.	2.0	11
251	Air-promoted selective hydrogenation of phenol to cyclohexanone at low temperature over Pd-based nanocatalysts. Science China Chemistry, 2017, 60, 1444-1449.	8.2	11
252	Low-Temperature Fabrication of Phase-Pure α-FAPbI3 Films by Cation Exchange from Two-Dimensional Perovskites for Solar Cell Applications. Energy & Fuels, 0, , .	5.1	11

#	Article	IF	CITATIONS
253	Shell-Isolated Nanoparticle-Enhanced Luminescence of Metallic Nanoclusters. Analytical Chemistry, 2020, 92, 7146-7153.	6.5	10
254	Title is missing!. Journal of Inclusion Phenomena and Macrocyclic Chemistry, 2001, 40, 121-124.	1.6	9
255	Mo-Decorated Ni ₃ N Nanostructures for Alkaline Polymer Electrolyte Fuel Cells. ACS Applied Nano Materials, 2021, 4, 11473-11479.	5.0	9
256	A nanoparticulate polyacetylene-supported Pd(II) catalyst combining the advantages of homogeneous and heterogeneous catalysts. Chinese Journal of Catalysis, 2015, 36, 1560-1572.	14.0	8
257	Mechanisms for CO oxidation on Fe(<scp>iii</scp>)–OH–Pt interface: a DFT study. Faraday Discussions, 2014, 176, 381-392.	3.2	7
258	Catalysis Selects Its Own Favorite Facets. CheM, 2019, 5, 1935-1937.	11.7	7
259	Chemoselective Hydrogenation of Nitroaromatics at the Nanoscale Iron(III)–OH–Platinum Interface. Angewandte Chemie, 2020, 132, 12836-12840.	2.0	7
260	Synthesis, structural characterization and ab initio calculation of dipyridyltetraazathiapentalene: a highly conjugative polycyclic molecule with hypervalent N–S–N bond. Journal of Molecular Structure, 2002, 610, 265-270.	3.6	6
261	A facile one-pot synthesis of supercubes of Pt nanocubes. Science China Chemistry, 2016, 59, 452-458.	8.2	6
262	Intimate Interfacial Interaction between Aminoâ€Modified Ti ₅ Clusters and BiVO ₄ towards Efficient Photoelectrochemical Water Splitting. ChemNanoMat, 2019, 5, 1110-1114.	2.8	6
263	Ag 44 (EBT) 26 (TPP) 4 Nanoclusters With Tailored Molecular and Electronic Structure. Angewandte Chemie, 2021, 133, 9120-9126.	2.0	6
264	Surface Reconstruction and Reactivity of Platinum–Iron Oxide Nanoparticles. Journal of Physical Chemistry C, 2014, 118, 28861-28867.	3.1	5
265	Acetyleneâ€Mediated Synthesis of Supported Pt Nanocatalyst for Selective Hydrogenation of Halonitrobenzene. ChemNanoMat, 2018, 4, 518-523.	2.8	5
266	Surface Coordination Decouples Hydrogenation Catalysis on Supported Metal Catalysts. CCS Chemistry, 2023, 5, 1215-1224.	7.8	5
267	Enhanced Surface Ligands Reactivity of Metal Clusters by Bulky Ligands for Controlling Optical and Chiral Properties. Angewandte Chemie, 2021, 133, 13007-13013.	2.0	4
268	Non-contact biomimetic mechanism for selective hydrogenation of nitroaromatics on heterogeneous metal nanocatalysts. Science China Chemistry, 2022, 65, 726-732.	8.2	4
269	Pd Nanoparticles Encapsulated in Hollow Mesoporous Aluminosilica Nanospheres as an Efficient Catalyst for Multistep Reactions and Size-Selective Hydrogenation. Acta Chimica Sinica, 2013, 71, 334.	1.4	3
270	Stabilizing Catalytic Pt-OH-Fe(III) Interfaces by Mesoporous TiO ₂ with Rich Surface Hydroxyl Groups. Acta Chimica Sinica, 2018, 76, 617.	1.4	3

#	Article	IF	CITATIONS
271	Regulating the Deposition of Insoluble Sulfur Species for Room Temperature Sodium-Sulfur Batteries. Chemical Research in Chinese Universities, 2022, 38, 128-135.	2.6	3
272	Structural Engineering of Heterometallic Nanoclusters. Frontiers of Nanoscience, 2015, , 73-102.	0.6	2
273	Amine facilitates the synthesis of silica-supported ultrasmall bimetallic nanoparticles. Science China Materials, 2018, 61, 1129-1131.	6.3	2
274	Lithium Batteries: Stable Nanoâ€Encapsulation of Lithium Through Seedâ€Free Selective Deposition for Highâ€Performance Li Battery Anodes (Adv. Energy Mater. 7/2020). Advanced Energy Materials, 2020, 10, 2070031.	19.5	2
275	Selective Nanocatalysis. ChemNanoMat, 2018, 4, 431-431.	2.8	1
276	Electrochemical Reduction of Nitrogen to Ammonia by Pd‣â€Mo Nanosheets on Hydrophobic Hierarchical Graphene Support. ChemElectroChem, 0, , .	3.4	1
277	Tertiary Chiral Nanostructures from Câ^'Hâ‹â‹F Directed Assembly of Chiroptical Superatoms. Angewandte Chemie, 2021, 133, 22585-22590.	2.0	1
278	Carbon monoxide-assisted shape control of Pd and Pt nanocrystals. Scientia Sinica Chimica, 2012, 42, 1525.	0.4	1
279	Cu-Containing Polyoxotitanate Cluster as a Catalyst Precursor for Understanding the Importance of Cu(II)–TiOx Interface on Selective Catalytic Reduction of NO. Journal of Cluster Science, 2023, 34, 255-260.	3.3	1
280	Cluster and Non-Cluster Based Open Framework Indium Chalcogenides. Materials Research Society Symposia Proceedings, 2002, 726, 1.	0.1	0
281	Pushing Up the Size Limit of Chalcogenide Supertetrahedral Clusters: Two- and Three-Dimensional Photoluminescent Open Frameworks from (Cu5In30S54)13- Clusters ChemInform, 2003, 34, no.	0.0	0
282	Synthetic Design of Crystalline Inorganic Chalcogenides Exhibiting Fast-Ion Conductivity ChemInform, 2004, 35, no.	0.0	0
283	Three-Dimensional Frameworks of Gallium Selenide Supertetrahedral Clusters ChemInform, 2004, 35, no.	0.0	Ο
284	Pentasupertetrahedral Clusters as Building Blocks for a Three-Dimensional Sulfide Superlattice ChemInform, 2004, 35, no.	0.0	0
285	Na5(In4S) (InS4)3×6H2O, a Zeolite-Like Structure with Unusual SIn4 Tetrahedra ChemInform, 2005, 36, no.	0.0	Ο
286	The Interface Chemistry Between Chalcogenide Clusters and Open Framework Chalcogenides. ChemInform, 2005, 36, no.	0.0	0
287	Two-Dimensional Organization of [ZnGe3S9(H2O)]4- Supertetrahedral Clusters Templated by a Metal Complex ChemInform, 2005, 36, no.	0.0	0
288	Special topic on strategies for developing energy-related physical chemistry. Science China Chemistry, 2017, 60, 1377-1378.	8.2	0

#	Article	IF	CITATIONS
289	The Inorganic Chemistry of Nanoparticles. Inorganic Chemistry, 2021, 60, 4179-4181.	4.0	0
290	A 3D open-framework indium telluride and its selenide and sulfide analogues. Angewandte Chemie - International Edition, 2002, 41, 1959-61.	13.8	0
291	Strain creates excellent catalysts for electrolyzers. Joule, 2021, 5, 3072-3074.	24.0	0